

# Equilibrium configurations from gravitational collapse

Pankaj S. Joshi,<sup>1,\*</sup> Daniele Malafarina,<sup>1,†</sup> and Ramesh Narayan<sup>2,‡</sup>

<sup>1</sup>*Tata Institute of Fundamental Research, Homi Bhabha Road, Colaba, Mumbai 400005, India*

<sup>2</sup>*Harvard-Smithsonian Center for Astrophysics, 60 Garden Street, Cambridge, MA 02138, USA*

We develop here a new procedure within Einstein's theory of gravity to generate equilibrium configurations that result as the final state of gravitational collapse from regular initial conditions. As a simplification, we assume that the collapsing fluid is supported only by tangential pressure. We show that the equilibrium geometries generated by this method form a subset of static solutions to the Einstein equations, and that they can either be regular or develop a naked singularity at the center. When a singularity is present, there are key differences in the properties of stable circular orbits relative to those around a Schwarzschild black hole with the same mass. Therefore, if an accretion disk is present around such a naked singularity it could be observationally distinguished from a disk around a black hole.

PACS numbers: 04.20.Dw, 04.20.Jb, 04.70.Bw

Keywords: Gravitational collapse, black holes, naked singularity

## I. INTRODUCTION

It is well known that any spherical distribution of non-interacting particles (thus in the absence of pressure), cannot sustain itself against the pull of its own gravitational field and must undergo complete gravitational collapse. The final outcome of such a dust collapse is either a black hole or a naked singularity, depending on the initial density configuration and velocity distribution of the particles [1]. In recent years, from the study of gravitational collapse in a wide variety of scenarios — self-similar collapse [2], scalar fields [3], perfect fluids [4] and other general forms of matter fields — it has emerged that black holes and naked singularities have both to be considered as possible final outcomes of complete collapse of a massive matter cloud in general relativity [5]. This is true also for alternative theories of gravity such as  $f(R)$  gravity and Lovelock gravity [6].

When non-vanishing pressures are present within the matter cloud – a physically more realistic scenario than dust – complete gravitational collapse is not the only possible final state. Hence, a question of much physical interest is, if and under what conditions can we have equilibrium configurations that originate from dynamical gravitational collapse within general relativity. In fact, we know that equilibrium non-singular gravitating systems exist in nature, e.g., planets, stars, galaxies, all of which form via gravitational collapse, and that these objects are of great significance from the perspective of both theory and observations.

We show here that the gravitational collapse of a matter cloud with non-vanishing tangential pressure, from regular initial data, can give rise to a variety of equilibrium configurations as the collapse final state. We consider here, for the sake of simplicity and clarity, the case of collapse with non-zero tangential pressure and vanishing radial pressure. While such a simplified model represents in some sense an idealized example, the case of a more realistic matter source, for example composed of a perfect fluid (with both radial and tangential pressure), can also be investigated and its equilibrium configurations will be reported separately in a future work. Collapse with only tangential pressure provides a relatively transparent structure (mainly because the mass function is conserved as we explain below), and this case is of much interest in its own right, since it reveals a rich array of possibilities. Therefore it is important and useful to study and understand these simpler models in order to figure out the possibilities that they offer on the collapse final states.

Models with vanishing radial pressure were first investigated by Datta in the special case where the matter cloud is composed of counter-rotating particles in the so called Einstein cluster geometry [7]. Over the past years, these models have been studied in detail in order to characterize the final outcome of complete gravitational collapse in terms of black holes and naked singularities [8]. We use here the general formalism developed in [9] to study the dynamical evolution of a massive matter cloud that collapses from regular initial data. We develop a technique and procedure that allows us to investigate when such a collapse can halt to form an equilibrium configuration. We show that from such a collapse process static configurations can arise which are either regular or singular at the center. We then investigate a particular toy model belonging to this class which presents a central naked singularity and we study the physical properties of an accretion disk in this spacetime.

The main noteworthy feature of the work presented here is that it shows the existence of solutions in which naked singularities arise from a dynamical process of gravitational collapse, starting from regular initial conditions. This makes the models useful

---

\*Electronic address: psj@tifr.res.in

†Electronic address: daniele.malafarina@polimi.it

‡Electronic address: rnarayan@cfa.harvard.edu

and interesting from a physical point of view since many other naked singular geometries that are usually investigated within general relativity are not obtained from the dynamical evolution of a collapsing cloud with regular initial data (although we note that there exist some much discussed examples of ways to overspin a Kerr black hole, thus turning it into a naked singularity by dropping spinning extended bodies through the horizon, see for example [10]). We point out here that although we deal with an idealized toy model, where the singularity is approached asymptotically, physically it can be interpreted as a slowly evolving collapse scenario where the central density is increasingly high (to a point where quantum effects would become relevant), and which is always visible to faraway observers. At later and later times, as the gravitational collapse evolves, the collapse model will be arbitrarily close to the idealized final static configuration, with the rate of collapse becoming arbitrarily small. Therefore such a ‘freezing’ of the dynamics as  $t$  grows allows us to neglect the collapse at a late enough time when the central region has achieved an extremely high density. At this late time, the approximation to a static configuration holds to a high degree of accuracy, and it is meaningful to study its physical properties, e.g., the nature of an accretion disk in the static configuration.

The properties of circular orbits for a non-rotating source sustained only by tangential pressure, as discussed here, differ considerably from corresponding results evaluated for the Kerr spacetime (see for example [11]). Furthermore, the objects we study will have different optical properties in terms of shadows and gravitational lensing compared to well studied analogues in other static and stationary geometries. In fact, it has been shown that whenever a photon sphere is present, as is the case in certain Kerr geometries, the effects of gravitational lensing make a naked singularity indistinguishable from a black hole [12]. In the model presented here, we find naked singularities with no photon sphere, thus leaving open the possibility to distinguish such objects from a black hole.

While the arguments presented above provide a number of motivations for the present study, the main objective of this work is to show the existence of models in which asymptotically static spacetimes with and without naked singularities arise as a result of dynamical gravitational collapse from regular initial configurations. It is briefly shown that observational features e.g., of an accretion disk, in such models can be quite different from those of a Schwarzschild black hole, though a more detailed investigation of the properties of accretion disks, including a parameter study of energy flux and luminosity, is deferred to a future work.

In section II, we give a brief overview of the general formalism to describe the dynamical evolution of a matter cloud sustained by tangential pressure. This formalism can be applied to the case of collapse, expansion, bounce or asymptotic equilibrium. In section III we impose the condition that the system asymptotes to a state of equilibrium, and we then analyze under what circumstances a collapsing cloud can settle to such a static limit. Section IV is then devoted to the analysis of a toy model for which the stable circular orbits and related physical properties of interest are presented. This is used to establish when, and in what manner, such models can be observationally distinguished from a black hole. Finally, in section V we highlight the main results and indicate perspectives for future research.

## II. GRAVITATIONAL COLLAPSE

The spherically symmetric spacetime metric describing a dynamical gravitational collapse can be written as,

$$ds^2 = -e^{2\nu} dt^2 + \frac{R'^2}{G} dr^2 + R^2 d\Omega^2, \quad (1)$$

where  $\nu$ ,  $R$  and  $G$  are functions of the comoving time  $t$  and the comoving (Lagrangian) radial coordinate  $r$ . In the case of vanishing radial pressure the energy-momentum tensor is given by  $T_0^0 = \rho$ ,  $T_1^1 = 0$ ,  $T_2^2 = T_3^3 = p_\theta$ , and the Einstein equations take the form

$$p_r = -\frac{\dot{F}}{R^2 \dot{R}} = 0, \quad (2)$$

$$\rho = \frac{F'}{R^2 R'}, \quad (3)$$

$$p_\theta = \frac{1}{2} \rho R \frac{\nu'}{R'}, \quad (4)$$

$$\dot{G} = 2 \frac{\nu'}{R'} \dot{R} G. \quad (5)$$

In the above,  $F$  is the Misner-Sharp mass, which describes the amount of matter enclosed by the shell labeled by  $r$ , and is given by

$$F = R(1 - G + e^{-2\nu} \dot{R}^2). \quad (6)$$

Equation (2), which results from the assumption of pure tangential pressure, immediately implies that  $F = F(r)$ , and so the mass interior to any Lagrangian radius  $r$  is conserved throughout the evolution. Therefore, at all times the metric describing the

evolving cloud can be matched to an exterior Schwarzschild solution with a total mass  $M_{\text{TOT}}$  at a boundary  $r = r_b$ , which corresponds to a time-dependent physical radius  $R_b(t) = R(r_b, t)$  [13].

We note that it is also possible to consider a more general collapse problem where we allow for non-zero radial pressure. In that case, the considerable simplification of being able to match to Schwarzschild may no longer be possible. However, matching to a generalized Vaidya spacetime is always possible for any general type I matter field as also for fields with non-zero radial pressure, subject to satisfying energy conditions and other reasonable physical regularity conditions. We shall consider such a more general situation separately, but we focus here on the simpler case of zero radial pressures since it offers considerable clarity and transparency on the role that pressure plays in the dynamical evolution of gravitational collapse. This also allows us to see clearly how the presence of pressure permits equilibrium solutions, as opposed to the case of dust where such solutions are never possible. Models with non-zero tangential pressure have been of much interest in the past as mentioned above, though this interest was mainly focused on finding the collapse final states in terms of black holes or naked singularities.

There is a scaling degree of freedom available in the definition of the physical radius  $R$ . Using this we introduce a scaling function  $v(r, t)$  defined by

$$R(r, t) = r v(r, t), \quad v(r, t_i) = 1, \quad (7)$$

where the latter condition simply states that  $R = r$  at the initial time  $t = t_i$  from which the collapse develops. In the following we assume that no shell-crossing singularities, defined by  $R' = 0$ , occur during the evolution. These are supposed to be weak singularities that arise due to the collision of different radial shells and would be removable by a suitable change of coordinates. To avoid shell-crossing singularities we must impose that  $R' > 0$  during the evolution. This in turn implies that the weak energy conditions are satisfied for positive pressures during collapse whenever  $F' > 0$ .

Our main procedure now for evolving the gravitational collapse is as follows. We have six unknowns, namely  $\rho$ ,  $p_\theta$ ,  $\nu$ ,  $G$ ,  $F$  and  $R$ , and four Einstein equations, so we have the freedom to choose two free functions. Once we specify the initial data for the above six functions at an initial epoch  $t = t_i$  and specify the two free functions, the system is closed and the Einstein equations then evolve the collapse to any future time. Typically, we may choose the free functions to be the mass function  $F(r)$ , which specifies the initial mass which is conserved for the cloud (from which the energy density can be obtained from equation (3)), and the tangential pressure  $p_\theta$ . Then, given the initial values, the future evolution is fully determined by the Einstein equations [14]. We note that, while in the present case the mass function is time independent and is chosen once and for all, the pressure depends on  $r$  and  $t$  via  $v(r, t)$  as  $p_\theta = p_\theta(r, v)$ . Hence a global choice for the pressure at all times has to be supplied, which then fully fixes the evolution of the system. One could, for example, begin by choosing  $F = M_0 r^3$ , which corresponds to a matter cloud that is initially perfectly homogeneous (constant density). It is then known that, for certain classes of choices of the evolution of  $p_\theta$ , a complete gravitational collapse would terminate in either a black hole or a naked singularity final state [8]. On the other hand, for certain other choices of the pressure, a bouncing behaviour for the cloud may result, where the initial collapse is reversed to turn into an expansion [15]. It is thus the choice we make for  $p_\theta$  that determines which way the collapse develops and evolves in future: Whether it will be a continual collapse to either a black hole or a naked singularity, or there will be a bounce at some stage, or it will settle into an equilibrium final configuration as we discuss here.

We note that actually any choice of  $p_\theta$  is equivalent to a choice of a constitutive equation of state for the matter, and vice-versa. In fact, the relation between the energy density and the tangential pressure is given implicitly by equation (4),

$$k(r, v) \equiv \frac{p_\theta}{\rho} = \frac{1}{2} R \frac{\nu'}{R'}, \quad (8)$$

and so  $p_\theta$  in general need not have an idealized form such as a linear or polytropic function of  $\rho$ . In fact, it is reasonable to suppose that the collapsing system will go through very different regimes, moving from its initial low density and weak gravitational field configuration to later stages where the density and gravitational fields might be extremely high. This would be reflected in the constitutive equation being, in general, a function of  $r$  and  $t$ , taking into account how the matter content changes during the evolution.

From equations (4) and (5), we can solve for  $\nu$  and  $G$  to obtain

$$\nu(r, t) = 2 \int_0^r k \frac{R'}{R} d\tilde{r} + y(t), \quad (9)$$

$$G(r, t) = b(r) e^{4 \int_0^1 \frac{k}{v} d\tilde{v}}. \quad (10)$$

We ignore the function  $y(t)$ , which comes from integrating equation (4), since it can be absorbed in a redefinition of the time coordinate  $t$ . The free function  $b(r)$ , which comes from integrating equation (5), is related to the velocity profile of the particles (it is easy to check that in the pressureless case we get  $G = b$ ). The only unknown that remains finally is the metric function  $R$ , which is the physical radius for the matter cloud and which is given by the solution of the differential equation for  $\dot{R}$  provided

by equation (6). The interior spacetime metric during collapse can then be written as

$$ds^2 = -e^{4 \int_0^r k \frac{R'}{R} d\bar{r}} dt^2 + \frac{R'^2}{b(r) e^{4 \int_v^1 \frac{k}{v} d\bar{v}}} dr^2 + R^2 d\Omega^2 . \quad (11)$$

In the present case with the spacetime metric given as above, while certain explicitly solved interior models such as the Einstein cluster are available, we note that in general obtaining explicit solutions in fully integrated form for the Einstein equations is rather difficult except in the simplest cases. It is also not always necessary. What we really need here for our purpose is, assuming regular behaviour of the free functions and the initial data, information about the structure of the dynamical collapse. In fact, the behaviour of a collapse solution can often be inferred in many cases without having to explicitly carry out the full integrations.

### III. EQUILIBRIUM CONFIGURATIONS

We investigate the following question here: For what choices or classes of the pressure  $p_\theta(r, v)$  (or equivalently  $p_\theta(r, t)$ ), does a cloud that collapses from regular initial conditions approach asymptotically an equilibrium configuration with a static spacetime geometry? In the following, given the freedom to choose the tangential pressure function  $p_\theta$ , we construct classes of models in which the pressure balances the attraction of gravity in the asymptotic final state, thereby obtaining final equilibrium configurations. This is subject to physical conditions such as the positivity of energy density and the regularity of the initial data.

For any fixed  $r$ , the equation of motion (6) can be written in terms of  $v$  in the form of the following effective potential,

$$V(r, v) = -\dot{v}^2 = -e^{2\nu} \left( \frac{M}{v} + \frac{G-1}{r^2} \right) , \quad (12)$$

where the function  $M(r)$  is defined by  $F = r^3 M(r)$ , and a suitable choice of this function implies that the Misner-Sharp mass is well-behaved at the center of the cloud (*i.e.*, non-singular and without cusps). In the Newtonian analogy, the negative of the effective potential describes the weighted kinetic energy of the particles in the shell labeled by  $r$ . Notice that, since  $F$  does not depend on  $t$ , it must be the same throughout the collapse and in the final equilibrium state.

From the above equations it is clear that any static configuration or bounce cannot at all arise in pressureless dust collapse. This is seen immediately from the fact that for dust  $\dot{v}^2 = M(r)/v + f(r)$ . Therefore, if  $\dot{v} < 0$  at some time, *i.e.*, once collapse has begun,  $\dot{v} < 0$  continues to be satisfied at all later times. Further, if the density is not zero, then  $\ddot{v} = 0$  cannot be achieved at any later time. The continual dust collapse thus inevitably terminates in a spacetime singularity as the collapse final state, which is either covered within an event horizon thus forming a black hole, or is a naked singularity. This final state either way is determined by the nature of the initial data from which the collapse evolves. The addition of non-zero pressures changes the situation. In particular, it also introduces a degree of freedom that can be used to balance the gravitational attraction to obtain a static final equilibrium configuration, as we show below.

In order for the system to reach a static configuration where collapse stabilizes, we require both the velocity and the acceleration of the in-falling shells to go to a vanishing value as the collapse progresses in future. We therefore need the limiting conditions,

$$\dot{v} = \ddot{v} = 0, \quad (13)$$

which are equivalent to  $V = V_{,v} = 0$ , where

$$V_{,v} = e^{2\nu} \left( \frac{M}{v^2} - \frac{G_{,v}}{r^2} \right) - 2\nu_{,v} e^{2\nu} \left( \frac{M}{v} + \frac{G-1}{r^2} \right) . \quad (14)$$

As the collapse progresses in time, the evolution metric function  $v(t, r)$  approaches in the limit an equilibrium value  $v = v_e(r)$ . The effective potential can be considered as a function of  $v$  for any fixed shell  $r$ , so from the conditions (13) we obtain the limiting equilibrium configuration  $v_e(r)$ .

We note that in the comoving coordinates that we have used here, the final equilibrium, *i.e.*, the static limit, is reached in the limit of the comoving time  $t$  going to infinity. If we linearize the effective potential  $V$  near the equilibrium configuration  $v_e$ , we can write it as  $V(v) = H(r)^2 (v - v_e)^2$  for a certain function  $H < 0$  that can be obtained from the second derivative of  $V$ . Therefore we get  $dv/(v - v_e) = H(r) dt$ , or  $(v - v_e) = \exp[H(r)(t - t_i)]$ , which implies  $v \rightarrow v_e$  as  $t \rightarrow +\infty$ . It is possible that there might exist some reparametrization of  $t$  that allows the singularity to appear in a finite time. But it is not necessary to find such a coordinate change explicitly as we prefer to work with comoving coordinates, which have a clear physical interpretation and appeal.

Once  $M(r)$ , or equivalently the mass function  $F(r)$ , is chosen, by imposing the conditions (13) we obtain two equations that fix the behaviour of  $G$  and  $G_{,v}$  at equilibrium in terms of the equilibrium solution  $v_e(r)$ ,

$$G_e(r) = G(r, v_e(r)) = 1 - \frac{r^2 M(r)}{v_e(r)}, \quad (15)$$

$$(G_{,v})_e = G_{,v}(r, v_e(r)) = \frac{M(r)r^2}{v_e^2}, \quad (16)$$

where the velocity profile  $b(r)$  that appears in equation (10) has been absorbed into  $G_e(r)$ . From equation (3) evaluated at equilibrium, we obtain the energy density at equilibrium,

$$\rho_e(r) = \frac{3M + rM'}{v_e^2(v_e + rv_e')}, \quad (17)$$

while the tangential pressure can be written as

$$p_{\theta e} = \frac{1}{4} \rho_e v_e \frac{(G_{,v})_e}{G_e} = \frac{1}{4} \frac{r^2 M(3M + rM')}{v_e^2(v_e + rv_e')(v_e - r^2 M)}. \quad (18)$$

In any gravitational collapse that begins from regular initial conditions, *i.e.*, that has a regular mass function  $F(r)$ , and evolves towards a final equilibrium state, we have the freedom to choose the final configuration via the function  $v_e(r)$ . Once we choose  $F(r)$  and  $v_e(r)$ , these two functions fully determine all other quantities in the final equilibrium:  $\rho_e(r)$ ,  $G_e(r)$ ,  $(G_{,v})_e(r)$  and  $p_{\theta e}(r)$ . While this fully specifies the final state, we still have the freedom to choose how the system evolves between the initial and final configurations. As stated earlier, the collapse evolution is fully fixed by choosing  $F(r)$  and  $p_{\theta}(r, v)$ , one of which, namely the mass function  $F(r)$ , we have already chosen. Thus, in order to go to the desired final equilibrium configuration as collapse limit, the class of allowed pressures  $p_{\theta}(r, v)$  is to be so chosen that we have  $p_{\theta}(r, v) \rightarrow p_{\theta e}(r)$  as  $t \rightarrow \infty$ , where the equilibrium pressure  $p_{\theta e}(r)$  was determined by the choice of the free function  $v_e(r)$ , as indicated above. For this entire class of  $p_{\theta}$  evolutions, the dynamical gravitational collapse will necessarily go in the asymptotic limit to an equilibrium spacetime geometry, which is defined by  $F(r)$  and  $v_e(r)$ .

Thus, we can finally write the metric (11) at equilibrium as,

$$ds_e^2 = -e^4 \int_0^r \frac{p_{\theta e} R_e'}{\rho_e R_e} d\tilde{r} dt^2 + \frac{R_e'^2 (\rho_e + 4p_{\theta e})}{\rho_e} dr^2 + R_e^2 d\Omega^2, \quad (19)$$

where  $R_e(r) = rv_e(r)$  is the physical radius of the Lagrangian shell  $r$  in the final equilibrium configuration. A dynamical solution of the Einstein field equations, as represented by the metric (11) with  $F(r)$  fixed, and with the class of pressures  $p_{\theta}(r, t)$  chosen such that  $p_{\theta} \rightarrow p_{\theta e}$  (or equivalently choosing a function  $v(r, t)$  such that  $v \rightarrow v_e$ ), will therefore tend to a final equilibrium metric of the form (19), where in the final state all the functions depend only on  $r$ .

In principle, the above equilibrium metric, which is the final state of collapse, is not required to be necessarily regular at the center. In fact we can see from equation (3) that since  $M$  is finite at  $r = 0$ , whenever we have  $v_e(0) = 0$ , the energy density at equilibrium diverges at  $r = 0$  and the equilibrium metric presents a central spacetime singularity. Clearly, this singularity has been achieved as the result of collapse from regular initial data that respect the energy conditions and it is somehow similar to those arising in complete gravitational collapse, though in this case the outer shells do not fall into the singularity but halt at a finite radius, thus creating a static compact object.

We see from the above that in order to fix completely the behaviour of  $p_{\theta}$  at equilibrium, we need to give the explicit form at equilibrium of  $G$  and  $G_{,v}$  and both the equilibrium conditions, namely  $\dot{v} = 0$  and  $\ddot{v} = 0$ , are necessary as well as sufficient for such a purpose. The freedom to choose the tangential pressure as above in the evolving collapse phase allows for different effective potentials to have different equilibrium configurations. On the other hand, we can reverse the reasoning and choose a certain equilibrium configuration  $v_e(r)$ , which implies a specific  $p_{\theta e}$ . We can then select the class of tangential pressures with proper limit such that they give rise to that specific effective potential (see Fig. 1).

If an equilibrium configuration with a singularity at the center is achieved as the limit of gravitational collapse, it is important to check under what conditions the singularity will not be covered by an event horizon. In the static limit, this simply means that the boundary where the cloud matches the vacuum Schwarzschild exterior has a radius greater than the Schwarzschild radius. Therefore, from the boundary condition at equilibrium we obtain a condition for the absence of trapped surfaces at equilibrium. In order for the region near the center to be not trapped, we must have  $F/R < 1$ . In the final equilibrium state, writing  $G$  in terms of energy density and pressure, we have

$$\frac{F}{R_e} = 1 - G_e = \frac{4p_{\theta e}}{\rho_e + 4p_{\theta e}}, \quad (20)$$

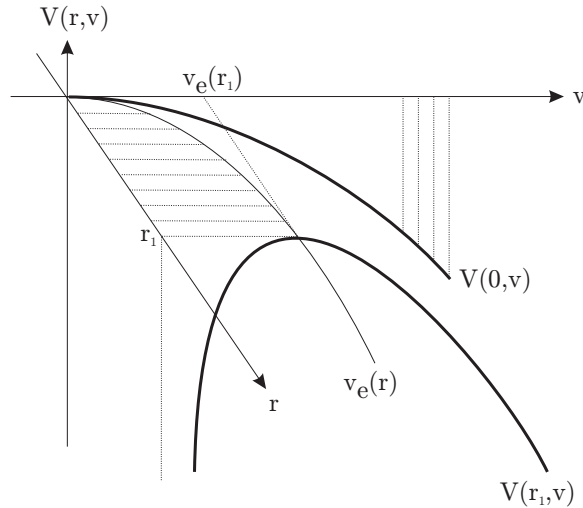


FIG. 1: The conditions for equilibrium given in equation (13) require that, for each  $r$ , the effective potential  $V(r, v)$  as a function of  $v$  should have a maximum, and further that the value of the potential at the maximum must be zero. Then,  $V(r, v) = 0$  implicitly defines  $v_e(r)$ .

which is obviously smaller than unity for positive energy density and positive  $p_{\theta e}$ . Thus, we obtain the interesting result that any central singularity that forms in the final equilibrium configuration via the collapse dynamics described in this paper is always a naked singularity. This is not surprising since we are describing dynamical evolution from regular initial data without trapped surfaces. This means that at the initial time  $t_i$  the center of the cloud is not trapped. Since the evolution remains regular, with the singularity arising as  $t$  goes to the asymptotic limit as the system reaches equilibrium, we can, in principle, choose any time slice to be the initial time. This implies that during the whole evolution the center of the cloud is not trapped and so the central singularity that appears in the final equilibrium is naked.

It is relevant to mention here that static interior solutions of the Schwarzschild metric have been studied in the past and static interiors supported by only tangential pressures were given by Florides [16], who wrote the most general metric in this case and found solutions depending on the choice of the free function  $F(r)$ . A static spherically symmetric line element depends only on the physical radius  $R$ , and it is easy to verify that it can be obtained from the metric (19), once a suitable change of coordinates  $R = R(r)$  is made. It therefore follows that the class of equilibrium configurations we have obtained here belongs to the family of static metrics given by Florides. The Einstein equations are easily rewritten in this case. The metric functions  $G$  and  $\nu$  in the static tangential pressure case are then given by

$$G(R) = 1 - \frac{F(R)}{R}, \quad 2\nu_{,R} = \frac{F(R)}{R^2 G}, \quad (21)$$

and equation (4) becomes a definition for the tangential pressure.

The important point is, the entire family of static tangential pressure solutions described by Florides can be obtained from gravitational collapse as the asymptotic equilibrium limit of collapse, by using the procedure we outlined here.

The physical relevance of such equilibrium configurations comes from the fact that in the case of a singularity at the center, as the comoving time  $t$  increases, the collapse slows down and the central density increases arbitrarily high. For sufficiently large values of  $t$  the static models do therefore approximate the collapsing cloud to an arbitrarily high degree of accuracy (see Fig. 2).

As noted earlier, the naked singularity here, when present in the final equilibrium configuration, is achieved only asymptotically by the collapsing cloud as the comoving time goes to infinity. In the collapsing matter cloud that approaches the equilibrium, there is no singularity at the center at any finite time  $t$ . Even when the divergence of the energy density occurs at an infinite comoving time, what is important to note is that the ultra-high density region that develops at the center of the collapsing cloud continues to be always visible and never trapped. This is the region where classical relativity may eventually break down at high enough densities and quantum effects might occur and dominate. This phase is always obtained in a finite but large enough time, before the actual singularity of the equilibrium. It is the visibility of such a region during collapse, which approaches in the limit the equilibrium model with an actual naked singularity at the center, which is the main reason for our study of the physical properties of such objects. In contrast, we know that in the case of collapse to a black hole, the ultra-high density regions are always necessarily hidden inside the event horizon after a certain stage in the collapse, and any Planck scale physics that might occur close to the singularity is invisible to distant observers.

The basic point we make here is: At later and later times, as the collapse progresses, the interior metric of the collapsing matter cloud becomes arbitrarily close to that of the static configuration metric. This is the sense in which the static or equilibrium configuration is approached to a higher and higher degree of accuracy as the dynamical collapse proceeds. Thus the collapse

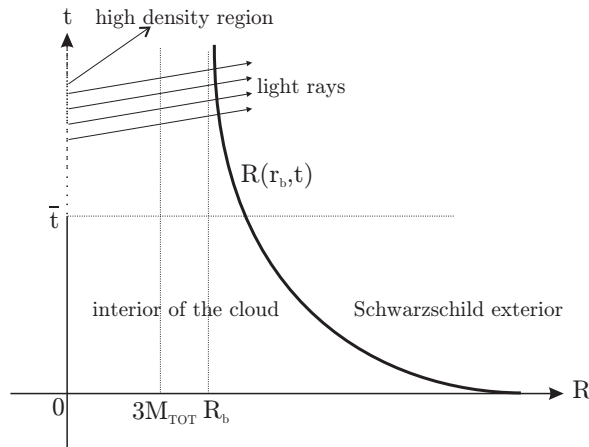


FIG. 2: The collapsing cloud approaches asymptotically the equilibrium configuration. For  $t > \bar{t}$  the central density grows to arbitrarily high values. No trapped surfaces are present at any time. Light rays would escape the strong gravity region, reach the boundary and then propagate to the exterior. As  $t$  grows the collapsing cloud approximates more and more the static model. The boundary remains larger than the photon sphere for the Schwarzschild spacetime at all times.

eventually freezes as time evolves, with the velocities and acceleration of the collapsing shells becoming arbitrarily small, approaching a vanishing value. The dynamical collapse asymptotes to the static tangential pressure model to arbitrary precision at late times, and so the static model is the limiting configuration to which it converges.

We have thus obtained here a wide family of gravitational collapse solutions that lead to equilibrium configurations in the final state. This family of solutions has the following degrees of freedom: Firstly, we have the freedom to choose any form of the equilibrium function  $v_e(r)$ . Then, corresponding to that  $v_e(r)$ , we have a wide family of tangential pressures  $p_\theta(r, v)$ , or equivalently  $p_\theta(r, t)$ , which we can choose from, all of which give the same final equilibrium state as a result of dynamical collapse.

#### IV. PHYSICAL APPLICATIONS

In this section, we study the physical properties of a particular static naked singularity toy model which is supported by tangential pressure. The aim is to study differences between black hole and naked singularity configurations and to understand observational signatures that might be used to distinguish naked singularities and black holes of the same mass. We focus on the nature of stable circular orbits in a chosen metric and consider the properties of accretion disks.

In the following, we discuss a specific model where we choose the mass function to be  $F(r) = M_0 r^3$  such that the regularity conditions are fulfilled during collapse. The divergence of the energy density in the limit of the equilibrium configuration is then achieved by a choice of  $v_e(r)$  such that  $v_e(0) = 0$ . As an example, we consider  $v_e(r) = cr^\alpha$  where, for simplicity, we set  $c = 1$  (thus imposing a scaling in the boundary conditions). It is easy to verify that the value  $\alpha = 0$  corresponds to a regular solution with positive density, namely the ‘constant density’ interiors first studied by Florides. On the other hand,  $\alpha > 0$  gives  $v_e(0) = 0$  and implies the presence of a naked singularity at  $r = 0$  in equilibrium. These singular interior models differ from other regular interiors for Schwarzschild in the behaviour of the density and curvatures near the center (see for example [17] for other regular interior solutions with perfect fluid sources and/or cosmological constant). The choice of  $v_e(r)$  determines the mapping between the physical radius  $R$  and the comoving coordinate  $r$  in the static metric,  $R(r) = rv_e(r) = r^{\alpha+1}$ , and this, together with the choice of  $F(r)$ , fixes the static solution. In the specific toy model considered here, we have

$$F(r) = M_0 r^3, \quad v_e(r) = r^\alpha, \quad F(R) = M_0 R^{\frac{3}{\alpha+1}}. \quad (22)$$

From the Einstein equations we obtain expressions for the equilibrium density  $\rho_e$  and pressure  $p_{\theta e}$ ,

$$\rho_e = \frac{3M_0}{(\alpha+1)} \frac{1}{R^{\frac{3\alpha}{\alpha+1}}}, \quad (23)$$

$$p_{\theta e} = \frac{3M_0^2}{4(\alpha+1)} \frac{R^{\frac{2-4\alpha}{\alpha+1}}}{\left(1 - M_0 R^{\frac{2-\alpha}{\alpha+1}}\right)}. \quad (24)$$

Different values of  $\alpha$ , which correspond to different choices of  $F(R)$ , lead to different behaviours for the pressure as  $r \rightarrow 0$ . We see that  $\alpha < 1/2$  implies  $p_{\theta e} \rightarrow 0$ , while  $\alpha > 1/2$  implies  $p_{\theta e} \rightarrow +\infty$ ; the transition value  $\alpha = 1/2$  implies  $p_{\theta e} \rightarrow \text{const}$ .

In general, to understand the properties of accretion disks in the static tangential pressure spacetimes as given by equation (21), let us consider test particles in circular orbits. Without loss of generality, we take the orbits to be in the equatorial plane ( $\theta = \pi/2$ ). Since the static metric is independent of  $t$  and  $\phi$ , we have two conserved quantities, the energy per unit mass,  $E = u_t = e^{2\nu}(dt/d\tau)$ , and the angular momentum per unit mass,  $\ell = u_\phi = R^2(d\phi/d\tau)$ . The normalization condition  $u^\alpha u_\alpha = -1$  then gives

$$\frac{1}{G} \left( \frac{dR}{d\tau} \right)^2 - E^2 e^{-2\nu} + \left( 1 + \frac{\ell^2}{R^2} \right) = 0. \quad (25)$$

For circular orbits, we set  $dR/d\tau = 0$ , so we require the remaining terms in the above equation to add up to zero. In addition, their sum should achieve an extremum at radius  $R$ . This gives the two conditions

$$E^2 = 2e^{2\nu} \left( \frac{R - F}{2R - 3F} \right), \quad (26)$$

$$\frac{\ell^2}{R_b^2} = \frac{F}{2R - 3F} \left( \frac{R}{R_b} \right)^2, \quad (27)$$

where  $R_b$  is the physical radius corresponding to the boundary of the matter cloud in the final equilibrium state. It is to be noted that since we are considering accretion disks which rotate freely in a metric that describes an internal fluid, we have to assume that the fluid constituting the naked singularity is weakly interacting with the matter constituting the accretion disk, so that the particles in the disk can have circular geodesic motion.

From equations (26) and (27) we find that, for  $R_b < 3M_{\text{TOT}}$ , both the quantities  $E^2$  and  $\ell^2$  become negative, thus indicating that the accretion disk particles must have imaginary energy and angular momentum to move on circular geodesics. This result is true also for perfect fluid interiors describing static sources of the Schwarzschild spacetime. Furthermore, for  $R < 2.5M_{\text{TOT}}$ , the sound speed within the cloud becomes superluminal, which is unphysical. For all these reasons, in the following we focus on models with  $R_b > 3M_{\text{TOT}}$ .

In order to understand the properties of these naked singularity models better and to compare them with the Schwarzschild black hole case, we now consider a specific example, viz., models with  $\alpha = 2$ . In this case, both the energy density and the pressure diverge at the center as  $R^{-2}$ . From the Misner-Sharp mass, we see that at the boundary  $2M_{\text{TOT}}/R_b = M_0$ . Thus the energy density is given by  $\rho_e = M_0/R^2$  and the pressure satisfies a linear equation of state,  $p_{\theta e} = k\rho_e$ , with  $4k = M_0/(1 - M_0)$ . In this simple model, the condition to avoid an event horizon is specifically  $M_0 < 1$ . Furthermore, to satisfy the weak energy condition, we must have  $k \geq -1$ , which corresponds to  $M_0 \leq 4/3$ . The effective sound speed  $c_\theta$  is given by  $c_\theta^2 = p_{\theta e}/\rho_e = k$ , and if we want this to be less than unity we then require  $M_0 < 4/5$ .

From the Einstein equations we find  $2\nu(R) = \ln [CR^{M_0/(1-M_0)}]$ , where  $C$  is an integration constant that can be evaluated from the boundary condition. Thus we obtain

$$e^{2\nu(R)} = (1 - M_0) \left( \frac{R}{R_b} \right)^{M_0/(1-M_0)}. \quad (28)$$

The complete solution for the metric in the interior  $R < R_b$  is then given by,

$$ds_e^2 = -(1 - M_0) \left( \frac{R}{R_b} \right)^{\frac{M_0}{1-M_0}} dt^2 + \frac{dR^2}{1 - M_0} + R^2 d\Omega^2. \quad (29)$$

This metric matches smoothly to a Schwarzschild spacetime in the exterior  $R \geq R_b$ ,

$$ds^2 = - \left( 1 - \frac{M_0 R_b}{R} \right) dt^2 + \frac{dR^2}{(1 - M_0 R_b/R)} + R^2 d\Omega^2. \quad (30)$$

We thus have a one-parameter family of static equilibrium solutions parametrized by  $M_0$  (in principle, there is a second parameter  $R_b$ , but this is simply a scale). Each member of this family of solutions has a naked singularity at the center. As described earlier, these solutions can be obtained as the end state of dynamical collapse from regular initial conditions with  $F(r) = M_0 r^3$ , by choosing the evolution function  $v(r, t)$  such that it asymptotes to the required  $v_e(r) \propto r^2$  as  $t \rightarrow \infty$  (see equation (22)).

In order to specify the nature of the central singularity, we note that the outgoing radial null geodesics in the spacetime above are given by,

$$\frac{dR}{dt} = (1 - M_0) \left( \frac{R}{R_b} \right)^{\frac{M_0}{2(1-M_0)}}. \quad (31)$$



It is then easy to check that there are light rays escaping from the singularity (for all values of  $M_0 < 2/3$ ). In fact from the above equation which gives,

$$t(R) = \frac{2R_b^{\frac{M_0}{2(1-M_0)}}}{2-3M_0} R^{\frac{2-3M_0}{2(1-M_0)}}, \quad (32)$$

we see immediately that the comoving time required by a photon to reach the boundary is  $t_b = 2R_b/(2-3M_0) < +\infty$ . It follows that there are future directed null geodesics in the spacetime which reach the boundary of the cloud, and which in the past terminate at the singularity, thus showing this to be a naked singularity. The density and spacetime curvatures would diverge in the limit of approach to the singularity in the past along these null trajectories, showing this to be a curvature singularity. The Kretschmann scalar for this naked singularity model, for the  $\alpha = 2$  case, is given by

$$K = \frac{1}{4} \frac{M_0^2(28 - 60M_0 + 33M_0^2)}{(M_0 - 1)^2 R^4}. \quad (33)$$

We see that the Kretschmann scalar diverges in the limit of approach to the central singularity. The spacetime is regular everywhere for all values of  $r > 0$ . A similar situation holds also for other models in this class of tangential pressure solutions. The divergence of curvatures at the center clarifies that this is a genuine spacetime singularity. Then the absence or otherwise of a trapped surface would determine whether this is a naked singularity or not, which again it is in this case, as we have shown above.

Circular geodesics for accretion disks in singular spacetimes without an event horizon have been studied in a variety of scenarios that include static and stationary spacetimes with and without a scalar field ([11] and see also [18]). The motion of test particles in circular orbits in a given spacetime is characterized by the existence of certain key parameters such as the photon sphere, the minimum radius for bound circular orbits and the minimum radius for stable circular orbits. As we shall see below the main features that stand out for our static toy model are the absence of an innermost stable circular orbit, meaning that stable orbits extend all the way to the singularity, and absence of the photon sphere. This marks a sharp contrast with similar analysis in some other naked singular static and stationary geometries where the presence of both a minimum radius for stable orbits and a photon sphere make the objects virtually indistinguishable from a black hole, at least as far as their optical properties are concerned (see [12]).

For the toy naked singularity model under consideration, the energy per unit mass  $E$  and angular momentum per unit mass  $\ell$  of the circular orbits may be obtained from equations (26) and (27). For  $R < R_b$ , we find,

$$E^2 = \frac{2(1-M_0)^2}{(2-3M_0)} \left( \frac{R}{R_b} \right)^{M_0/(1-M_0)}, \quad (34)$$

$$\frac{\ell^2}{R_b^2} = \frac{M_0}{(2-3M_0)} \left( \frac{R}{R_b} \right)^2. \quad (35)$$

If we want the circular orbit calculated above to be stable, we require in equation (25) that the term involving  $E^2$  should be less divergent as  $R \rightarrow 0$  compared to the term involving  $\ell^2$ . This then gives the following results for  $R < R_b$ :

$$\text{Stable circular orbits :} \quad M_0 \leq 2/3, \quad (36)$$

$$\text{Unstable circular orbits :} \quad M_0 > 2/3. \quad (37)$$

We see that, depending on the value of  $M_0$ , either all circular orbits in the interior of this naked singularity model are stable, or all are unstable. Note that, apart from having unstable circular orbits, models with  $M_0 > 2/3$  also give negative values of  $E^2$  and  $\ell^2$ .

For  $R \geq R_b$ , the metric is given by the Schwarzschild solution with mass  $M_{\text{TOT}} = M_0 R_b/2$ . Here we have well-known results for the stability of circular orbits, viz., orbits with  $R \geq 6M_{\text{TOT}}$  are stable, while those with  $R < 6M_{\text{TOT}}$  are unstable. Further, the space-time has closed circular photon orbits at  $R = 3M_{\text{TOT}}$  (assuming this radius is located outside  $R_b$ ).

The practical significance of the above results is related to the fact that a standard thin accretion disk can exist only at those radii where stable circular orbits are available [19]. Thus, for a Schwarzschild black hole of mass  $M_{\text{TOT}}$ , an accretion disk will have its inner edge at the innermost stable circular orbit at  $R = 6M_{\text{TOT}}$ . Inside this radius, the gas plunges or free-falls until it crosses the horizon. The existence of a well-defined disk inner edge [20], which is the basis for the well-known Novikov-Thorne model of a relativistic thin accretion disk around a black hole [19], will be reflected in the radiation spectrum emitted by the disk. Indeed, observations have confirmed the presence of such an edge in several cases [21]. Moreover, assuming that the central object is a black hole, the radius of the disk inner edge has been used to estimate the spin parameters of the black holes [22].

It is worth noting from equations (34) and (35) that both the energy per unit mass  $E$  and the angular momentum per unit mass  $\ell$  of the gas in the accretion disk vanish in the limit of  $R = 0$ . This means that no mass or rotation is added to the central

singularity by the accretion disk, whose particles radiate away or otherwise get rid of all their energy and angular momentum before reaching the singularity. It thus follows that the process of accretion does not affect the naked singularity, which can be considered stable in this respect. This is very different from what is expected to happen in the case of a rotating Kerr naked singularity, where the process of accretion of counter-rotating particles can spin down the object and turn it into a near-extremal black hole (see for example [23]).

We considered above several general physical features of the toy naked singularity model, many of which also apply to the general class of static tangential pressure models with a naked singularity. In general, the observational properties of accretion disks can be characterized in terms of the energy flux, luminosity, and also the spectrum of the emitted radiation. Such features have been analyzed recently within certain models with naked singularities which are present in extremal stationary Kerr space-time geometries (see e.g. [18]). Such studies might possibly help towards observationally distinguishing black holes from naked singularities. From such an investigation of different aspects of accretion disks we may be able to reveal the crucial features that make them different from the widely studied accretion disks in the Kerr spacetime. It has to be noted, however, that many of the models with static or stationary naked singularities, such as the Janis-Newman-Winicour (JNW) spacetime, Reissner-Nordstrom geometries with  $Q > M$  or superspinning Kerr geometries need not arise naturally from dynamical evolution in gravitational collapse under Einstein's equations. Our model, on the other hand, provides a dynamical framework through which a static compact object with a naked singularity at its core can be formed as the limit of gravitational collapse of a massive matter cloud with non-zero tangential pressure.

A detailed analysis of the properties of accretion disks for interior solutions with tangential pressure, both in the regular and singular cases, is beyond the scope of this paper and will be discussed in detail elsewhere. Our main purpose here is a comparison of these naked singularity objects which can form via collapse, with a Schwarzschild black hole of the same mass. Therefore, making use of the stability properties of circular orbits, we identify the following two distinct model regimes, each with its own accretion structure, as we discuss below:

- $M_0 \leq 1/3$ , i.e.,  $R_b \geq 6M_{\text{TOT}}$ :

In this case, the external Schwarzschild metric has stable circular orbits all the way down to the boundary  $R = R_b$  where it meets the interior metric of our naked singularity solution. Consequently, an accretion disk will follow the standard Novikov-Thorne disk solution down to  $R = R_b$ . Inside  $R_b$ , the interior metric allows stable circular orbits all the way down to  $R = 0$ . Thus, the disk will continue into the interior and will extend down to  $R = 0$ . In other words, the disk will have no inner edge. Assuming the matter cloud that makes up the naked singularity is transparent to radiation (we have already assumed that it does not interact with the gas in the accretion disk), a distant observer will receive radiation from all radii down to the center and the observed spectrum will obviously be very different from that seen from a disk around a black hole of the same mass. (We postpone detailed computation of the spectrum to a later investigation.) As an aside, note that this space-time has no circular null geodesics (photon sphere).

- $1/3 < M_0 \leq 2/3$ , i.e.,  $6M_{\text{TOT}} > R_b \geq 3M_{\text{TOT}}$ :

In this case, an accretion disk will follow the Novikov-Thorne solution down to  $R = 6M_{\text{TOT}}$ . Inside this radius, since circular orbits are unstable in the Schwarzschild space-time, the gas will plunge towards smaller radii. However, once the gas reaches the boundary of the interior solution at  $R = R_b$ , circular orbits are once again available. Hence, we expect the gas to shock and circularize at  $R = R_b$  and then to continue accreting along a sequence of stable circular orbits all the way down to  $R = 0$ . (We assume that the gas at  $R_b$  can get rid of its excess angular momentum by some means to the outer disk across the gap.) Since the accretion disk in this model consists of two distinct segments with a radial gap in between, we expect it to be observationally distinguishable from the previous case. Once again, there is no photon sphere in this space-time.

As we have mentioned before, the models with  $3M_{\text{TOT}} > R_b > 2M_{\text{TOT}}$  (corresponding to  $2/3 < M_0 < 1$ ) present unphysical and exotic properties that would indicate that the boundary of the final static configuration should be taken at a value larger than  $3M_{\text{TOT}}$ . We note that for the accretion regimes we considered above, which is the range as given by  $M_0 < 2/3$ , all reasonable physical properties for the matter fields are satisfied by the particles of the accretion disk.

The interesting point is that due to the absence of a photon sphere, naked singularity models with  $M_0 < 2/3$  are easily distinguishable from a black hole of the same mass. This opens up the possibility of using observational data on astrophysical black hole candidates to test for the presence of a naked singularity. The discussion here pertains only to the particular toy model with  $\alpha = 2$ . Models with other values of  $\alpha$ , or more generally, models in which  $v_e(r)$  is more complicated than a power-law in  $r$ , may well give other kinds of behavior that may be worth investigating.

A key quantity in the case of an accretion disk is the radiant energy flux as a function of radius. This is given by

$$f(R) = -\frac{\dot{m}}{\sqrt{-g}} \frac{\omega_{,R}}{(E - \omega\ell)^2} \int_{R_{in}}^R (E - \omega\ell)\ell_{,R} dR, \quad (38)$$

where  $R_{in}$  is the radius of the inner edge of the disk,  $\dot{m}$  is the mass accretion rate, which for steady state accretion is usually assumed to be constant, and  $\omega = d\phi/dt$  is the angular velocity of particles on circular orbits. For a Schwarzschild black hole,  $R_{in} = 6M_{\text{TOT}}$  and  $f(R)$  vanishes for smaller radii. This leads to well-known results that are widely used for modeling accretion disks observed in astrophysics. In the case of our naked singularity model, the inner edge of the disk is at  $R = 0$ .

Therefore, the flux continues to increase with decreasing  $R$ , diverging at  $R = 0$  (the integrated total luminosity observed at infinity is of course finite). The disk ends up being much more luminous as compared to the black hole case (see Fig. 3) and the two cases may be easily distinguished. The fact that  $f(R)$  diverges as  $R$  goes to zero is not surprising and is related to the presence of the singularity.

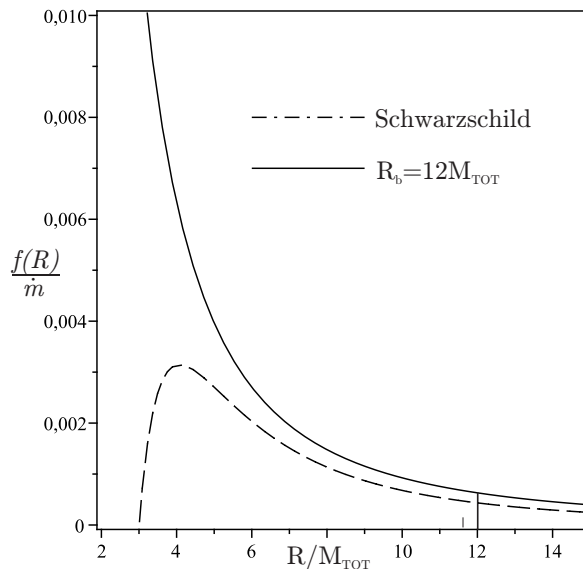


FIG. 3: Comparison between the radiant energy flux for an accretion disk around a Schwarzschild black hole with total mass  $M_{\text{TOT}}$  (dashed line), and for an accretion disk in the toy naked singularity model with the same mass and  $R_b = 12M_{\text{TOT}}$  (solid line).

Although we decided earlier to focus on models with  $M_0 < 2/3$ , for completeness we briefly discuss here the parameter range  $2/3 < M_0 < 1$ . For a model in this range, an accretion disk will follow the Novikov-Thorne solution down to  $R = 6M_{\text{TOT}}$ . The lack of stable circular orbits inside this radius will then cause the gas to plunge inwards. When the gas crosses  $R = R_b$ , there are still no stable circular orbits available (in contrast to the previous cases), so the gas will continue to plunge all the way down to  $R = 0$ . The accretion disk in this case is easily distinguishable from each of the previous two cases. However, for various reasons, it will most likely be indistinguishable from a standard Novikov-Thorne disk around a Schwarzschild black hole of mass  $M_{\text{TOT}}$ . Firstly, although the fate of the gas that reaches the naked singularity at the center is unclear, since this gas carries energy and angular momentum it will most likely modify the nature of the central singularity. Secondly, any radiation that is emitted from the singularity will not escape to infinity, as we showed earlier. Both arguments suggest that this model will behave for all practical purposes like a black hole. This regime is further divided into two subregimes since for  $4/5 \leq M_0 < 1$  we showed that the sound speed exceeds unity. Note that there is a photon sphere at the standard Schwarzschild location,  $R_{\text{photon}} = 3M_{\text{TOT}}$ .

All of the above discussion pertains to a model with  $\alpha = 2$ . It is interesting to note here, for the sake of a comparison, that in a model with  $\alpha = 0$ , which corresponds to a regular static solution with non-zero tangential pressure, there are again two different regimes according to where we take the boundary of the cloud. The first regime corresponds to  $R_b \geq 6M_{\text{TOT}}$ , and in this case there is no photon sphere and stable circular orbits extend all the way down to the regular center. In the second regime,  $6M_{\text{TOT}} > R_b \geq 3M_{\text{TOT}}$ , the matter in the accretion disk reaches the last stable circular orbit of the Schwarzschild spacetime at  $R = 6M_{\text{TOT}}$ , then plunges down to the boundary of the interior solution  $R = R_b$ , inside which stable orbits are again allowed down to the center. Again there is no photon sphere. The situation in this respect is thus similar to the first two cases studied above for the naked singularity model with  $\alpha = 2$ . The main difference for the  $\alpha = 0$  case is that particles in the accretion disk reach the regular center with non-vanishing energy (and vanishing angular momentum). It is useful to note that again, for  $R_b < 3M_{\text{TOT}}$  the energy and angular momentum have to be imaginary if a particle is to follow a circular geodesic, and for  $R_b < (5/2)M_{\text{TOT}}$  the effective sound speed surpasses unity while close to the boundary.

The naked singularity model presented here, which arises from the dynamical gravitational collapse of a massive matter cloud with non-zero tangential pressure, presents several interesting physical features some of which we have analyzed here. In particular, the accretion disk properties allow it to be distinguished observationally from a Schwarzschild black hole with the same mass. There are several other physical properties which are worth studying. Particular mention should be made to optical phenomena, where the toy naked singularity model discussed here will have quite different behavior compared to Kerr and certain other naked singularity spacetimes. The main important difference, as far as optical properties and gravitational lensing are concerned, is the following. All the other naked singularity models mentioned above and discussed earlier necessarily admit

the presence of a photon sphere for a certain range of the solution parameters involved. For example, the Reissner-Nordstrom spacetime with  $Q > M$ , which has a naked singularity, or the JNW naked singularity, necessarily admit a photon sphere when the quantities  $Q - M$  and the scalar charge  $\mu$  are respectively small enough. Such naked singularities have been termed as ‘weakly naked singular’ (see e.g. [12]), and are expected to be observationally indistinguishable from black holes, especially as far as their optical properties are concerned. As opposed to this, the tangential pressure naked singularity models presented here have no photon sphere as discussed above. Therefore these are necessarily ‘strongly naked singular’ and will be distinguishable always from black holes.

## V. CONCLUDING REMARKS

We have investigated here the equilibrium configurations that can be achieved from gravitational collapse of a spherical matter cloud with vanishing radial pressure. We showed that all static interiors of the Schwarzschild space-time with tangential pressure can be obtained as the limit of some model for dynamical gravitational collapse. These static interiors might be regular or they may have a naked singularity at the center.

The key important features of this model that distinguish it from other naked singular spacetimes are:

- The naked singularity is obtained via dynamical evolution of a matter cloud starting with regular initial data.
- For the particular class of toy models with  $\alpha = 2$ ,  $M_0 < 2/3$ , that we have focused on, the singularity is not destroyed by the infall of particles through an accretion disk and hence it is stable in this sense.
- Due to the absence of a photon sphere in these solutions, the singular spacetime is always optically distinguishable from a black hole with the same mass.

We also examined and noted here several physical properties and features of accretion disks in these naked singularity models, comparing them with those for a Schwarzschild black hole, and we noted how black holes and naked singularities will have observationally distinct signatures (e.g., see Fig. 3).

In analogy with the Newtonian case, although the equilibrium configurations we describe can be reached via a wide class of pressure evolutions, they sit at the maximum of the effective potential (see Fig. 1) and are expected to be unstable under small perturbations in the velocities. Therefore, tangential pressure models  $p_\theta(r, v)$  close to the ones leading to an equilibrium, but with a different asymptotic behaviour, will lead to either complete collapse or rebound. Nevertheless, the main point we wish to make is that static equilibrium configurations as a limit to gravitational collapse do arise and exist, and that the formalism for collapse in general relativity does not always imply that the matter cloud must necessarily collapse under its own gravity to a final singularity in a ‘short’ time. In fact, since the equilibrium configurations described here are reached only in the limit of  $t$  going to infinity, all neighbouring solutions (meaning those tangential pressure evolutions that have an asymptotic limit close to equilibrium) can be ‘long lived’ and could describe systems that evolve over an arbitrarily long time. In this sense, the equilibrium configurations investigated here constitute a valid toy model to describe ‘long lived’ dynamical models, where the collapse essentially ‘freezes’ as it evolves in time.

We investigated in section IV one specific static equilibrium solution ( $\alpha = 2$ ) with a naked singularity at the center, and we showed that the accretion properties of such an object can, in principle, be quite different from those of a Schwarzschild black hole. Other models with different values of the parameter  $\alpha$ , e.g., the Florides constant density interior solution ( $\alpha = 0$ ), or a different functional behaviour of  $v_e(r)$ , e.g.,  $v_e \simeq cr^\alpha$  only near  $r = 0$  and having a different radial variation away from the center, could be investigated as well. Other physical features such as gravitational lensing or the properties of the photon sphere could also be considered in more detail in order to have a better understanding of the physical nature and properties of these theoretical models.

Recently there has been some interest in the possibility of observationally distinguishing black holes from naked singularities. Most of these studies deal with naked singularities that are present in extremal stationary Kerr spacetimes and therefore need not arise naturally from dynamical evolution under Einstein’s equations. Our model, on the other hand, provides a dynamical framework through which a compact object with a naked singularity at its core can be formed.

The formalism developed in this paper might be applied in an astrophysical context to describe the final fate of gravitating objects collapsing under the force of their own gravity. There have been detailed investigations of the last stages of evolution of a massive star when all the radial shells of matter fall towards a central singularity to make a black hole. From the considerations described here other end-states are also possible, e.g. the system could asymptote to a static solution with or without a naked singularity. The class of static singular solutions might conceivably be of use to describe rare astrophysical phenomena.

### Acknowledgments

PSJ would like to thank Peter Biermann for discussions on the object-like and event-like character of singularities when they are visible.

- 
- [1] P. S. Joshi and I. H. Dwivedi, *Phys. Rev. D* **47**, 5357 (1993); B. Waugh and K. Lake, *Phys. Rev. D* **38**, 1315 (1988); R. P. A. C. Newman, *Class. Quantum Grav.* **3**, 527 (1986); D. Christodoulou, *Commun. Math. Phys.* **93**, 171 (1984); D. M. Eardley and L. Smarr, *Phys. Rev. D* **19**, 2239 (1979).
- [2] A. Ori and T. Piran, *Phys. Rev. Lett.* **59**, 2137 (1987); A. Ori and T. Piran, *Phys. Rev. D* **42**, 1068 (1990); T. Foglizzo and R. Henriksen, *Phys. Rev. D* **48**, 4645 (1993).
- [3] D. Christodoulou, *Ann. Math.* **140**, 607 (1994); R. Giambò, *Class. Quantum Grav.* **22**, 2295 (2005); S. Bhattacharya, R. Goswami and P. S. Joshi, *Int. J. Mod. Phys. D* **20**, 1123 (2011).
- [4] T. Harada, *Phys. Rev. D* **58**, 104015 (1998); T. Harada and H. Maeda, *Phys. Rev. D* **63**, 084022 (2001); R. Goswami and P. S. Joshi, *Class. Quantum Grav.* **19**, 5229 (2002); R. Giambò, F. Giannoni, G. Magli, P. Piccione, *Gen. Rel. Grav.* **36**, 1279 (2004); J. F. Villas da Rocha, A. Wang, *Class. Quantum Grav.* **17**, 2589 (2000).
- [5] S. L. Shapiro, S. A. Teukolsky, *Phys. Rev. Lett.* **66**, 994 (1991); S. L. Shapiro, S. A. Teukolsky, *Phys. Rev. D* **45**, 2006 (1992); K. Lake, *Phys. Rev. D* **43**, 1416 (1991); P. S. Joshi and A. Krolak, *Class. Quantum Grav.* **13**, 3069 (1996); P. S. Joshi, N. Dadhich, and R. Maartens, *Phys. Rev. D* **65**, 101501 (2002); R. Goswami and P. S. Joshi, *Phys. Rev. D* **76**, 084026 (2007).
- [6] A. H. Ziaie, K. Atazadeh and S. M. M. Rasouli, arXiv:1106.5638v1; A. H. Ziaie, K. Atazadeh and Y. Tavakoli, *Class. Quantum Grav.* **27**, 075016 (2010); N. Bedjaoui, P. G. LeFloch, J. M. Martin-García and J. Novak, *Class. Quantum Grav.* **27**, 245010, (2010); S. Ohashi, T. Shiromizu and S. Jhingan, *Phys. Rev. D* **84**, 024021 (2011); K. Zhou, Z. Y. Yang, D. C. Zou, R. H. Yue, arXiv:1107.2730.
- [7] B. K. Datta, *Gen. Rel. Grav.* **1**, 19 (1970); H. Bondi, *Gen. Rel. Grav.* **2**, 321 (1971); S. Jhingan and G. Magli, *Phys. Rev. D* **61**, 124006 (2000); T. Harada, H. Iguchi and K. Nakao, *Phys. Rev. D* **58**, 041502 (1998).
- [8] G. Magli, *Class. Quantum Grav.* **14**, 1937 (1997); G. Magli, *Class. Quantum Grav.* **15**, 3215 (1998); T. Harada, K. Nakao and H. Iguchi, *Class. Quantum Grav.* **16**, 2785 (1999); P. S. Joshi and R. Goswami, *Class. Quantum Grav.* **19**, 5229 (2002).
- [9] D. Malafarina and P. S. Joshi, *Int. J. Mod. Phys. D* **20**, 463 (2011); P. S. Joshi and D. Malafarina, *Phys. Rev. D* **83**, 024009 (2011).
- [10] F. de Felice and Y. Yunqiang, *Class. Quantum Grav.* **18**, 1235 (2001); A. Saa and R. Santarelli, *Phys. Rev. D* **84**, 027501 (2011).
- [11] Z. Stuchlík, *Bull. Astro. Inst. Czech.* **31**, 129 (1980); Z. Kovacs and T. Harko, *Phys. Rev. D* **82**, 124047 (2010).
- [12] K. S. Virbhadra and G. F. R. Ellis, *Phys. Rev. D* **65**, 103004 (2002); G. N. Gyulchev and S. S. Yazadjiev, *Phys. Rev. D* **78**, 083004 (2008); K. S. Virbhadra, D. Narasimha, and S. M. Chitre, *Astron. Astrophys.* **337**, 1 (1998); K. S. Virbhadra and C. R. Keeton, *Phys. Rev. D* **77**, 124014 (2008); C. Bambi and K. Freese, *Phys. Rev. D* **79**, 043002 (2009); Z. Stuchlík and J. Schee, *Class. Quantum Grav.* **27**, 215017 (2010).
- [13] W. Israel, *Nuovo Cemento B* **44**, 1 (1966).
- [14] P. S. Joshi and I. H. Dwivedi, *Class. Quantum Grav.* **16**, 41 (1999).
- [15] A. Mahajan and P. S. Joshi, *Gen. Rel. Grav.* **39**, 825 (2007).
- [16] P. S. Florides, *Proc. Roy. Soc. (London) Ser. A* **337**, 529 (1974).
- [17] K. Lake, *Phys. Rev. D* **67**, 104015 (2003); C. G. Böhrer, *Gen. Rel. Grav.* **36**, 1039 (2004); Z. Stuchlík, *Acta. Phys. Slov.* **50**, 219 (2000).
- [18] D. Pugliese, H. Quevedo and R. Ruffini, *Phys. Rev. D* **83**, 024021 (2011); T. Harada and M. Kimura, *Phys. Rev. D* **83**, 024002 (2011); C. Bambi, *Europhys. Lett.* **94**, 50002 (2011).
- [19] I. D. Novikov and K. S. Thorne, in *Black Holes*, eds. C. De Witt and B. S. De Witt, p343, Gordon and Breach, New York (1973); D. N. Page and K. S. Thorne, *Astrophys. J.* **191**, 499 (1974).
- [20] C. S. Reynolds and A. C. Fabian, *Astrophys. J.* **675**, 1048 (2008); R. Shafee, J. C. McKinney, R. Narayan, A. Tchekhovskoy, C. F. Gammie and J. E. McClintock, *Astrophys. J.* **687**, L25 (2008); R. F. Penna, J. C. McKinney, R. Narayan, A. Tchekhovskoy, R. Shafee and J. E. McClintock, *Mon. Not. Roy. astr. Soc.* **408**, 752 (2010); S. C. Noble, J. H. Krolik, J. F. Hawley, *Astrophys. J.* **711**, 959 (2010); A. K. Kulkarni, R. F. Penna, R. V. Shcherbakov, J. F. Steiner, R. Narayan, A. Sadowski, Y. Zhu, J. E. McClintock, S. W. Davis and J. C. McKinney, *Mon. Not. Roy. astr. Soc.* **414**, 1183 (2011).
- [21] J. F. Steiner, J. E. McClintock, R. A. Remillard, L. Gou, S. Yamada and R. Narayan, *Astrophys. J.* **718**, L117 (2010); J. F. Steiner, R. C. Reis, J. E. McClintock, R. Narayan, R. A. Remillard, J. A. Orosz, L. Gou, A. C. Fabian and M. A. P. Torres, *Mon. Not. Roy. astr. Soc.*, **416**, 941 (2011).
- [22] R. Shafee, J. E. McClintock, R. Narayan, S. W. Davis, L. X. Li and R. A. Remillard, *Astrophys. J.* **636**, L113 (2006); J. E. McClintock, R. Shafee, R. Narayan, R. A. Remillard, S. W. Davis and L. X. Li, *Astrophys. J.* **652**, 518 (2006); J. Liu, J. E. McClintock, R. Narayan, S. W. Davis and J. A. Orosz, *Astrophys. J.* **679**, L37 (2008); L. Gou, J. E. McClintock, J. Liu, R. Narayan, J. F. Steiner, R. A. Remillard, J. A. Orosz, S. W. Davis, K. Ebisawa and K. M. Schlegel, *Astrophys. J.* **701**, 1076 (2009); L. Gou, J. E. McClintock, J. F. Steiner, R. Narayan, A. G. Cantrell, C. D. Bailyn and J. A. Orosz, *Astrophys. J.* **718**, L122 (2010).
- [23] Z. Stuchlík, S. Hledík and K. Truparová, *Class. Quantum Grav.* **28**, 155017 (2011).